Spectroscopy, Electrochemistry, and Molecular Orbital Calculations of Metal-Free Tetraazaporphyrin, -chlorin, -bacteriochlorin, and -isobacteriochlorin

Hideya Miwa,[a] Elena A. Makarova,[b] Kazuyuki Ishii,[a] Evgeny A. Luk'yanets,*[b] and Nagao Kobayashi*[a]

Abstract: Metal-free tetraazachlorin (TAC), -bacteriochlorin (TAB), and -isobacteriochlorin (TAiB) were characterized by electronic absorption, magnetic circular dichroism (MCD), fluorescence, and time-resolved ESR (TR-ESR) spectroscopy, and by cyclic voltammetry. The results are compared with those of metal-free tetraazaporphyrin (TAP). The potential difference ΔE between the first oxidation and reduction couples decreases in the order TAP > TAiB > TAC > TAB. The splitting of both the Q and Soret bands decreases in the order TAB > TAC > TAP > TAiB. Corresponding to the split absorption bands, MCD spectra show a minus-to-plus pattern with increasing energy in both the Q and Soret regions, which suggests that the energy difference between the HOMO and second HOMO is larger than that between the LUMO and second LUMO. These spectroscopic properties and redox potentials were reproduced by molecular orbital calculations using the ZINDO/S Hamiltonian. The fluorescence quantum yields of the reduced species are much smaller than that of TAP. The zero-field splitting (ZFS) parameters D and E of the excited triplet states (T1) of these species decrease and increase, respectively, on going from TAP to TAC and further to TAB. The D and E values of TAiB are larger than those of the other species. The results are supported by the absence of interaction between the spin over reduced pyrrole moieties of the HOMO and over the LUMO, and by calculations of ZFS under a half-point-charge approximation.

Keywords: electrochemistry · EPR spectroscopy · porphyrinoids · semiempirical calculations · UV/Vis spectroscopy

Introduction

Porphyrin-related compounds are important for the preservation of life and have long fascinated many chemists and biologists.[1, 2] The in vivo functionality of porphyrins is largely attributable to their peculiar electronic structure, which is a 16-atom, 18-π-electron aromatic system, and D_{4h} symmetry. Porphyrins have a relatively weak Q band in the visible region and an intense Soret (B) band in the UV region, and these spectroscopic features have been described successfully by Gouterman's four-orbital model.[3] The chlorophylls and bacteriochlorophylls of green plants and bacteria are hydrogenated at C_β=C_β bonds of one or two pyrrole rings of porphyrin, and the resulting control of the position and intensity of the Q band allows efficient light gathering and energy transduction. Therefore, it is important to elucidate the influence of reduction and lowered symmetry of the π system on the electronic state of porphyrins. Compared to porphyrins, tetraazaporphyrins (TAPs) and phthalocyanines (Pcs), which are completely artificial compounds, have much more intense Q bands with allowed transition character. While the Pcs have already found use in a variety of fields,[4–6] the effect of peripheral substitution and modification of the π-conjugated system on the Q band is more pronounced in TAPs, which therefore have considerable potential as new functional materials. Here we report on experimental and theoretical studies on metal-free TAP and hydrogenated TAPs (i.e., TAC, TAB, and TAiB; Scheme 1) to clarify the effect of shrinkage and symmetry lowering of the π system. The electronic states and molecular orbital energies of these compounds were studied by cyclic voltammetry and by electronic absorption and MCD spectroscopy. In addition, the excited-state dynamics and electronic structure of the compounds after photoexcitation were investigated by fluorescence and TRESR spectroscopy. Molecular orbital (MO) calculations were used to interpret these spectroscopic and electrochemical properties. Although there are some previous publications on hydrogenated porphyrins, very little is known

[a] Prof. Dr. Dr. N. Kobayashi, H. Miwa, Dr. K. Ishii
Department of Chemistry
Graduate School of Science, Tohoku University
Sendai 980-8578 (Japan)
Fax: (+81) 22-217-7719
E-mail: nagaok@mail.cc.tohoku.ac.jp

[b] Prof. Dr. E. A. Luk'yanets, Dr. E. A. Makarova
Organic Intermediates and Dyes Institute
1/4 B. Sadovaya Str., 103787 Moscow (Russia)
Fax: (+7) 095-254-9866
E-mail: rmeluk@cityline.ru

  0947-6539/02/0805-1082 $ 17.50+.50/0

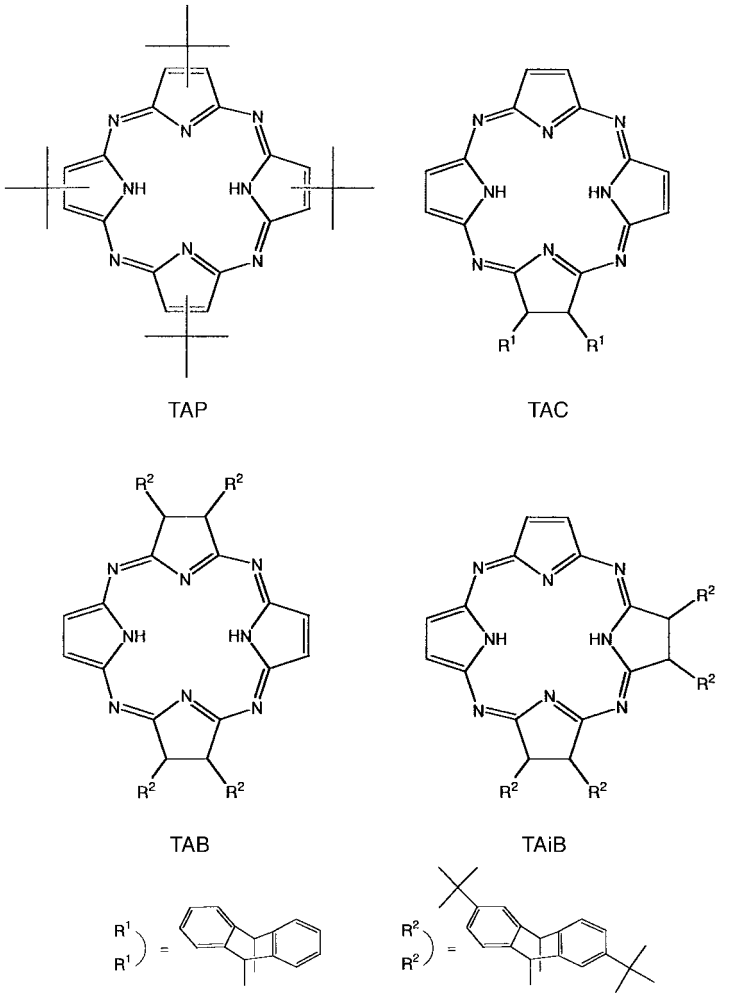

Scheme 1. Structures and abbreviations of the compounds studied here.

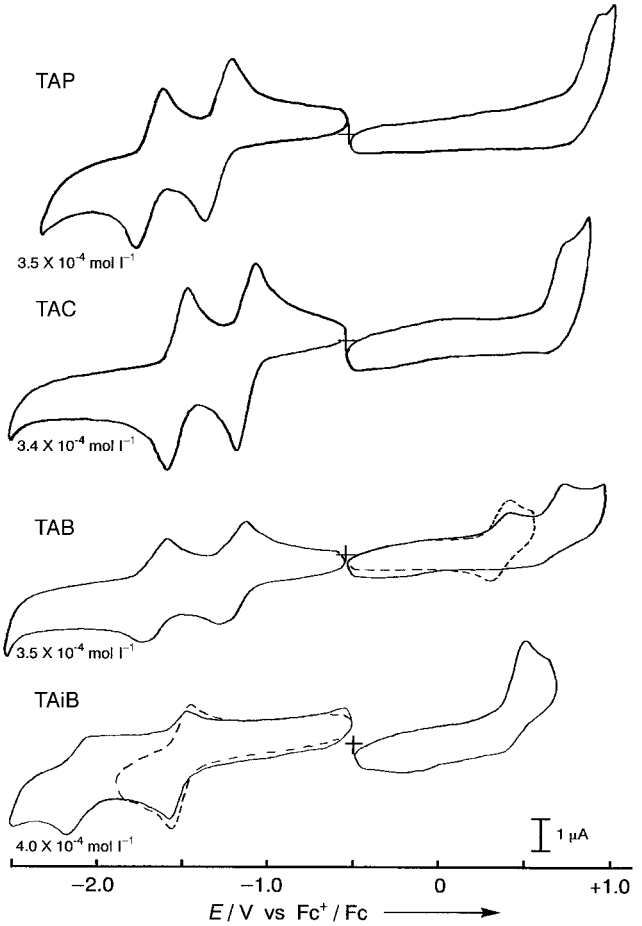

Figure 1. Cyclic voltammograms of TAP, TAC, TAB, and TAiB in *o*-dichlorobenzene with 0.1M TBAP. The scan rate was 50 mV s^{-1} for all compounds.

about the physicochemical properties of hydrogenated tetraazaporphyrins, mainly due to the difficulty of their synthesis.[7–13]

Results

Electrochemistry: Cyclic voltammograms were primarily recorded to obtain the relative energies of the HOMO and LUMO of the four compounds (Figure 1), and the electrochemical data are summarized in Table 1. Two reduction couples and one oxidation couple were observed for TAP, TAC, and TAiB, while an additional oxidation couple was also seen for TAB. In all cases, the first oxidation couples are irreversible; however, the first oxidation couple of TAB is reversible if the potential sweep is switched before reaching the second oxidation. All the reduction couples, except for those of TAiB, are reversible, while the first reduction couple of TAiB is reversible if the potential sweep is switched before reaching the second reduction. The first oxidation potentials shift cathodically with decreasing size of the π system (0.82, 0.64, 0.36, and 0.44 V for TAP, TAC, TAB, and TAiB, respectively). The first reduction potentials of TAC (−1.13 V) and TAB (−1.20 V) are more anodic than that of TAP (−1.31 V), while the first reduction potential of TAiB (−1.52 V) is more cathodic than for TAP. The potential difference ΔE between the first oxidation and reduction couples decreases in the order TAP > TAiB > TAC > TAB. These results indicate that the much lower HOMO–LUMO energy gap of TAC and TAB, compared with TAP, is due to destabilization of the HOMO and some stabilization of the LUMO, while the small decrease in the HOMO–LUMO energy gap of TAiB results from destabilization of both the HOMO and LUMO. Similar results have been reported for hydrogenated porphyrins.[14–19]

Table 1. Redox potentials (versus Fc^+/Fc) and diffusion coefficients D for TAP, TAC, TAB and TAiB in *o*-dichlorobenzene containing 0.1M TBAP.[a]

Species	$E^{2+/+}$	$E^{+/0}$	$E^{0/-}$	$E^{-/2-}$	D [cm^2 s^{-1}] [c]
TAP		0.82[b]	−1.31 (0.15)	−1.70 (0.15)	2.12×10^{-6}[d]
TAC		0.64[b]	−1.13 (0.10)	−1.53 (0.12)	3.12×10^{-6}[d]
TAB	0.66[b]	0.36 (0.11)	−1.20 (0.15)	−1.66 (0.15)	0.47×10^{-6}[e]
TAiB		0.44[b]	−1.52 (0.11)	−2.00[b]	0.52×10^{-6}[f]

[a] Numbers in parentheses indicate potential differences ΔE_p between cathodic and anodic peak potentials at a sweep rate of 50 mV s^{-1}. [b] The potentials are not clear in the cyclic voltammograms due to irreversibility; therefore, these potentials were determined from differential pulse voltammograms. [c] Diffusion coefficient. [d] Average values determined from the current peaks at the first and second reduction waves. [e] Average value determined from the current peaks at the first and second reduction waves and the first oxidation wave. [f] Value determined from the current peaks at the first reduction wave.

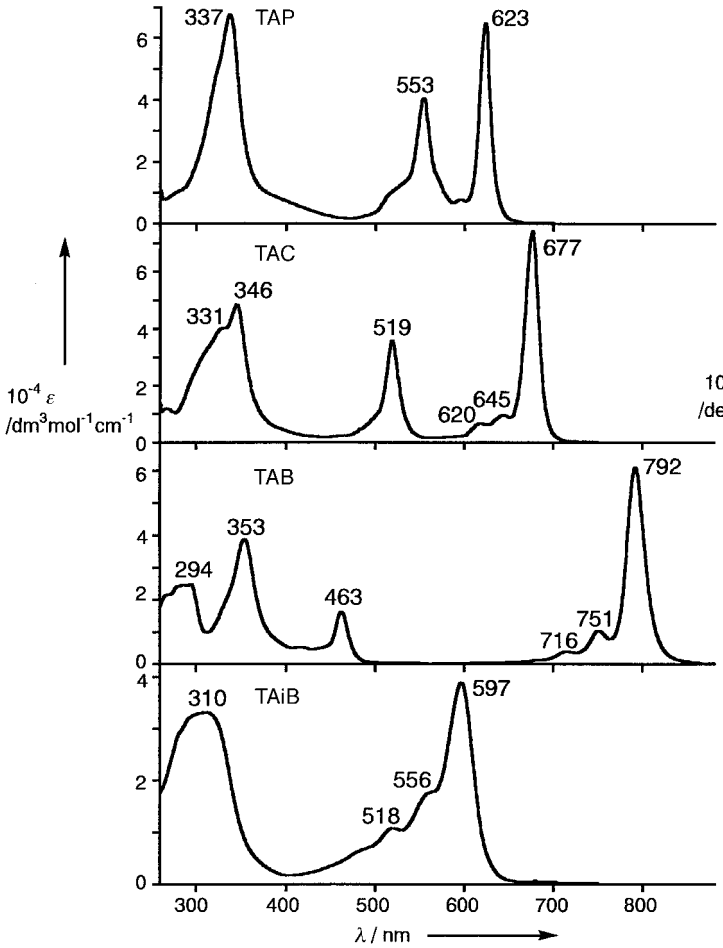

Figure 2. Electronic absorption spectra of TAP, TAC, TAB, and TAiB in chloroform.

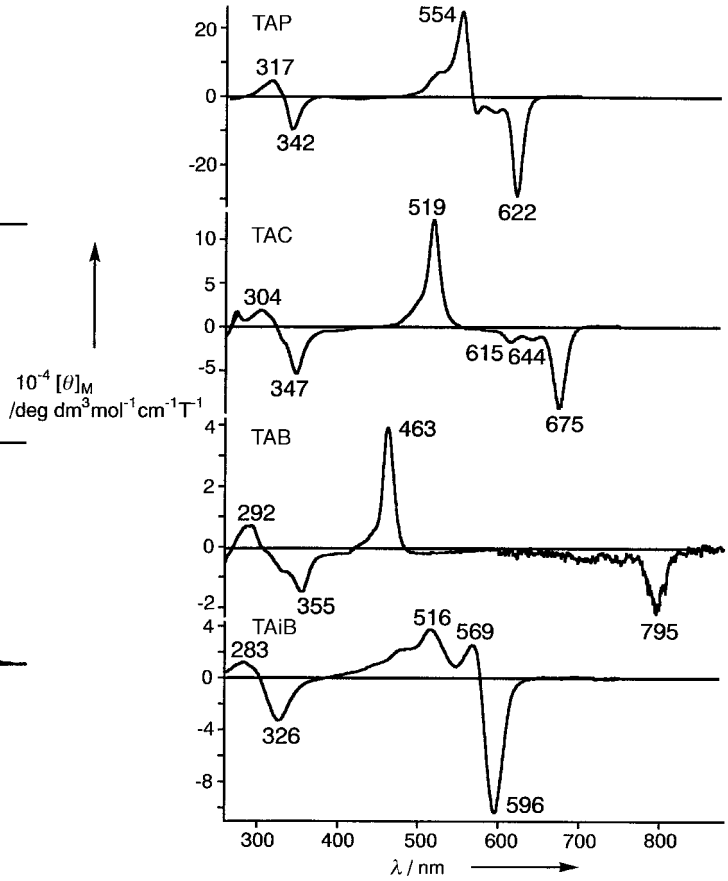

Figure 3. MCD spectra of TAP, TAC, TAB, and TAiB in chloroform. The applied magnetic field was 1.09 T.

Spectroscopy: *Absorption spectroscopy*: Figures 2 and 3 show the electronic absorption and MCD spectra, respectively, of the four compounds, and important data are summarized in Table 2. A large splitting of the Q bands is seen for TAP, TAC, and TAB, whereby the long-wavelength split peak Q1 is shifted to longer wavelength, and the short-wavelength peak Q2 to shorter wavelength, on going to TAC and TAB. This indicates that the splitting of the Q band increases with decreasing size of the π system (2040, 4490, and 9020 cm^{-1} for TAP, TAC, and TAB, respectively). Concomitantly, the ratio of the oscillator strength Q2/Q1 decreases with decreasing size of the π system (0.205/0.145 = 1.41, 0.162/0.200 = 0.81, and 0.0936/0.150 = 0.62 in the above order), that is, the intensity of the Q2 relative to the Q1 band decreases with increasing splitting energy. In contrast to these three compounds, TAiB, whose π system is equal in size to that of TAB, shows a broad Q absorption band that comprise one main peak at 597 and two shoulders at 556 and 518 nm. In the MCD spectrum of TAiB, a pair of oppositely signed *B* terms was detected at 596 nm, corresponding to the Q absorption peak and 569 nm; this indicates that the energy difference between Q1 and Q2 is at most ca. 800 cm^{-1}. The oscillator strength of this band (f = 0.362) is approximately equal to the sum of the strengths of the Q1 and Q2 bands in the other compounds. Since the HOMO–LUMO transition is regarded as the main configuration of the Q1 transition, the shift of the Q1 peak to longer wavelength with decreasing area of the π system is consistent with the cyclic voltammetry results (the decrease in ΔE). In the Soret band region, on the other hand, absorption peaks are seen at 337 nm for TAP, 346 with a shoulder at 331 nm for TAC, 353 and 294 nm for TAB, and 310 nm for TAiB. These results indicate that the splitting of the Soret band increases with decreasing area of the π system in a similar manner to the Q band, except in the case of TAiB. This is also seen in the MCD spectra (Figure 3).

Table 2. Electronic absorption and MCD data in $CHCl_3$.

Species	Electronic absorption λ/nm ($10^{-4}\,\varepsilon$ [dm^{3}mol^{-1}cm^{-1}])			MCD λ/nm ($10^{-4}[\theta]_M$ [deg dm^{3}mol^{-1}cm^{-1}T^{-1}])			
TAP	337 (6.73)	553 (4.03)	623 (6.50)	317 (4.60)	342 (−9.66)	554 (24.84)	622 (−29.08)
TAC	346 (4.83)	519 (3.57)	677 (7.42)	304 (1.90)	347 (−5.39)	519 (12.31)	675 (−9.29)
TAB	353 (3.87)	463 (1.62)	792 (6.11)	292 (0.70)	355 (−1.49)	463 (3.91)	795 (−2.14)
TAiB	310 (3.32)	597 (3.89)		283 (1.24)	326 (−3.32)	596 (−10.39)	

0947-6539/02/0805-1084 $ 17.50+.50/0 *Chem. Eur. J.* **2002**, *8*, No. 5

It is useful to compare the above spectroscopic changes with those seen in normal porphyrin systems, which do not contain *meso*-N atoms. Both the Q and Soret bands of normal porphyrins and TAPs are different in position and intensity: in general, an intense Soret and weak Q bands are found in the region of about 400–430 and 480–630 nm, respectively, for metal-free porphyrins.[20] In chlorins and bacteriochlorins, the position of the Soret band does not essentially change, but the Q1 and Q2 bands shift to about 610–650 and 520–590 nm and 720–780 and 490–580 nm, respectively, with an associated increase in the intensity of the Q1 band.[20] In isobacteriochlorins, the Soret and Q bands appear at around 360–430 and 550–640 nm, respectively.[21] On the whole, the spectra of bacteriochlorin and TAB are similar in shape, as are those of isobacteriochlorin and TAiB, although, relative to the corresponding porphyrins,[19] the Soret bands of the TAPs lie at shorter wavelengths (ca. 290–360 nm), and the splitting of the Q1 and Q2 bands is much larger.

MCD spectroscopy: Since there is no orbital degeneracy in these compounds due to the lack of a symmetry element higher than a threefold rotation axis, the MCD spectra exhibit only Faraday *B* terms.[22] The intensity of the Faraday *B* terms of the Q band decreases in the order TAP > TAC > TAB, and this reflects the degree of splitting of the Q band.[23–25] The sign pattern of the MCD *B* term bands of all compounds is $-/+$ with increasing energy, as is also seen for low-symmetry Pc derivatives,[26–30] although those of hydrogenated porphyrins were often inverted.[21, 31]

Michl predicted sign patterns of MCD Faraday *B* terms[32, 33] with increasing energy to be $+/-$ for ΔLUMO > ΔHOMO, and $-/+$ for ΔHOMO > ΔLUMO. The former pattern was often observed in the MCD spectra of unsymmetrical porphyrins such as chlorins.[21, 31] In porphyrin derivatives, ΔLUMO can frequently be larger than ΔHOMO, even after symmetry lowering, since the HOMO and second HOMO are almost degenerate under D_{4h} symmetry. In contrast, TAC and TAB showed the latter pattern, because ΔHOMO is larger than ΔLUMO in TAP derivatives, due to the strong stabilization of the second HOMO level when the *meso*-C atoms are replaced by electron-withdrawing N atoms.

Fluorescence spectroscopy: The decay kinetics in the lowest excited singlet states were examined by fluorescence measurements in chloroform (Figure 4). The fluorescence quantum yields were 0.29, 0.044, and 0.0047 for TAP, TAC, and TAiB, respectively, while no emission was observed for TAB. The fluorescence quantum yields of chlorins are generally higher than those of the corresponding porphyrins,[20] since the Q bands of chlorins are generally much more intense, and the natural radiative fluorescence rate is roughly proportional to the oscillator strength of the Q band. Although the oscillator strengths of the Q1 bands of TAC, TAB, and TAiB did not change significantly relative to that of TAP, the quantum yields of these hydrogenated azaporphyrins decrease markedly, and this suggests that nonradiative decay is promoted by dibenzobarreleno substituents and the energy gap law (note that the energy gap between the ground and lowest singlet excited states decreases with decreasing molecular symmetry, as illustrated by the position of the Q1 bands).

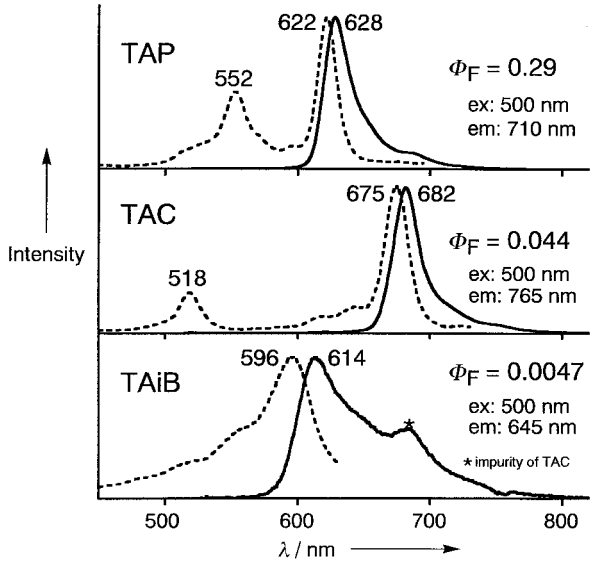

Figure 4. Fluorescence emission (solid lines) and excitation spectra (broken lines) of TAP, TAC, and TAiB in chloroform. Excitation wavelengths and emission wavelengths used to record excitation spectra and fluorescence quantum yields are shown.

TR-ESR spectroscopy: Figure 5 shows TRESR spectra recorded to obtain information on the electronic structure in the lowest excited triplet state. These spectra all exhibit an EEE/AAA polarization pattern characteristic of metal-free porphyrins and Pcs.[34–48] The E and A polarizations denote emission and absorption of microwaves, respectively, and result from nonequilibrium population of the triplet sublevels. The EEE/AAA polarization pattern is produced by selective intersystem crossing to the T1x and T1y sublevels (solid lines). Zero-field splitting parameters of these compounds are summarized in Table 3. The *D* value decreases in the order TAiB (1.38), TAP (0.99), TAC (0.855), TAB (0.833), and the *E* value increases in the order TAP (0.03), TAC (0.245), TAB (0.273), TAiB (0.34). The parameter *D* reflects an anisotropic distribution of unpaired electrons towards the out-of-plane axis *z* with respect to the distribution in the ring plane (*x*, *y* axes).[47] Therefore, the decrease in *D* on going from TAP to TAB is the opposite behavior to that expected for delocalization of the unpaired π electrons.[43] Similar results were reported for normal porphyrins, chlorins, and bacteriochlorins.[49] On the other hand, the parameter *E* reflects an

Table 3. Experimental ZFS parameters, sublevel population ratios, and ZFS calculated with a half-point-charge approximation.

Species	D [GHz]	D_{calcd} [GHz]	E [GHz]	E_{calcd} [GHz]	P_x:P_y:P_z[a]
TAP	0.990	0.801	0.030	0.152	0.5:0.5:0
TAC	0.855	0.790	0.245	0.188	0.35:0.65:0
TAB	0.833	0.647	0.273	0.250	0.65:0.35:0
TAiB	1.38	1.055	0.340	0.432	0.75:0.25:0

[a] $P_i (i = x, y, z)$ denotes anisotropic system crossing.

  0947-6539/02/0805-1085 $ 17.50+.50/0

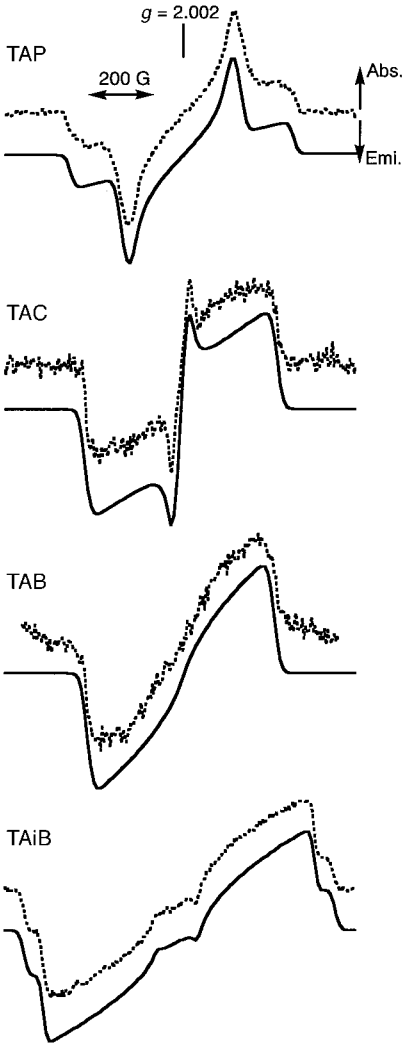

Figure 5. TR-ESR spectra of TAP, TAC, TAB, and TAiB (broken lines) together with their simulations (solid lines). Spectra were recorded at 20 K in toluene 0.9 μs after laser excitation.

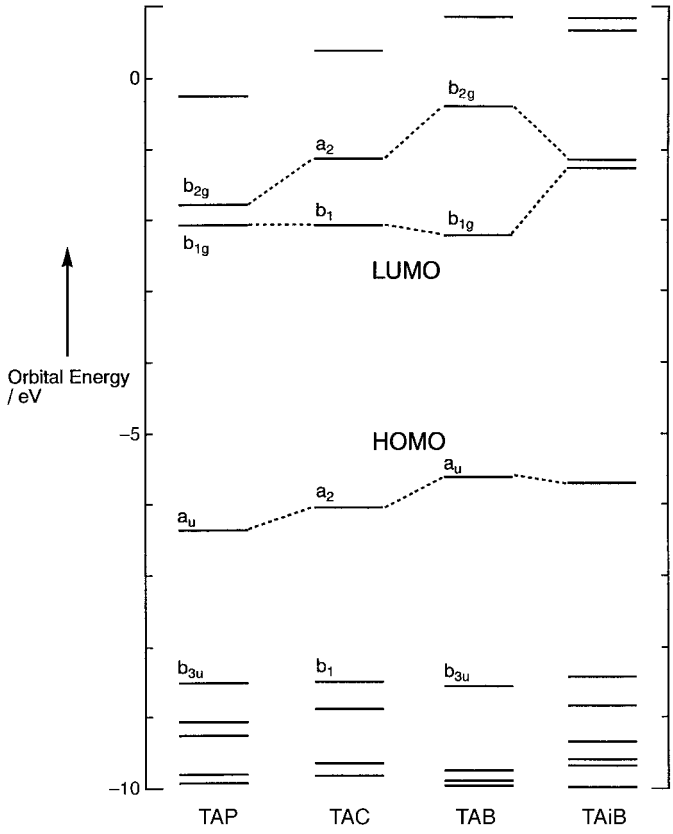

Figure 6. Partial molecular orbital energy diagram for TAP, TAC, TAB, and TAiB.

anisotropic distribution of unpaired electrons towards the in-plane axes *x* and *y*, so that the observed increase in *E* can be explained by symmetry lowering. The fact that the ZFS parameters of TAB and TAiB are quite different although their π systems are of similar size indicates that the large difference in electronic structure between TAB and TAiB can be attributed to their different molecular symmetries.

Discussion

Molecular orbital analysis: The energies of some frontier orbitals and the shapes of the four frontier orbitals, obtained by MO calculations within the framework of the ZINDO/S Hamiltonian,[50–52] are shown in Figure 6 and Figure 7, respectively. As seen in Figure 6, the HOMO is destabilized in the order TAP (−6.3641 eV), TAC (−6.0545 eV), TAiB (−5.6992 eV), and TAB (−5.6224 eV), while the second HOMO levels are hardly changed (−8.5246, −8.4959, −8.4322, and −8.5652 eV in the above order). The energy difference between the LUMO and second LUMO becomes larger with decreasing size of the π-conjugated system, mainly because of destabilization of the second LUMO, with the exception of TAiB, which has very small energy difference, even smaller than that of TAP, due to its adjacent pyrrole-reduced C_{2v}-type π system. These LUMO–second LUMO energy differences are much smaller than those between the HOMO and the second HOMO. The changes of the four orbital levels can be interpreted as follows. In TAP, the HOMO and second LUMO have some coefficients on the pyrrole rings that are hydrogenated in TAC and TAB, while the LUMO and second HOMO have very small coefficients. As a result, hydrogenation of the pyrrole rings affects the energy levels of the HOMO and second LUMO rather than the LUMO and second HOMO. The shapes of the LUMO and second LUMO of TAiB differ from those of the other compounds in having no nodal plane on the pyrrole nitrogen atoms, so that their energy changes cannot be explained by the same mechanism as in TAC and TAB. The results and explanation described above on the MO calculations are in agreement with the trends seen in the cyclic voltammetric measurements (Figure 1 and Table 1).

Excited singlet states: The changes in the Q bands of the compounds examined in this study (Figures 2 and 3) can be explained qualitatively by using a four-orbital model[3] including the HOMO (denoted as a_{1u} in D_{4h} symmetry), second HOMO (a_{2u}), LUMO, and second LUMO (e_{gx} and e_{gy}). In porphyrins, the HOMO and second HOMO levels are almost degenerate, so that the HOMO–LUMO and second

0947-6539/02/0805-1086 $ 17.50+.50/0 *Chem. Eur. J.* **2002**, *8*, No. 5

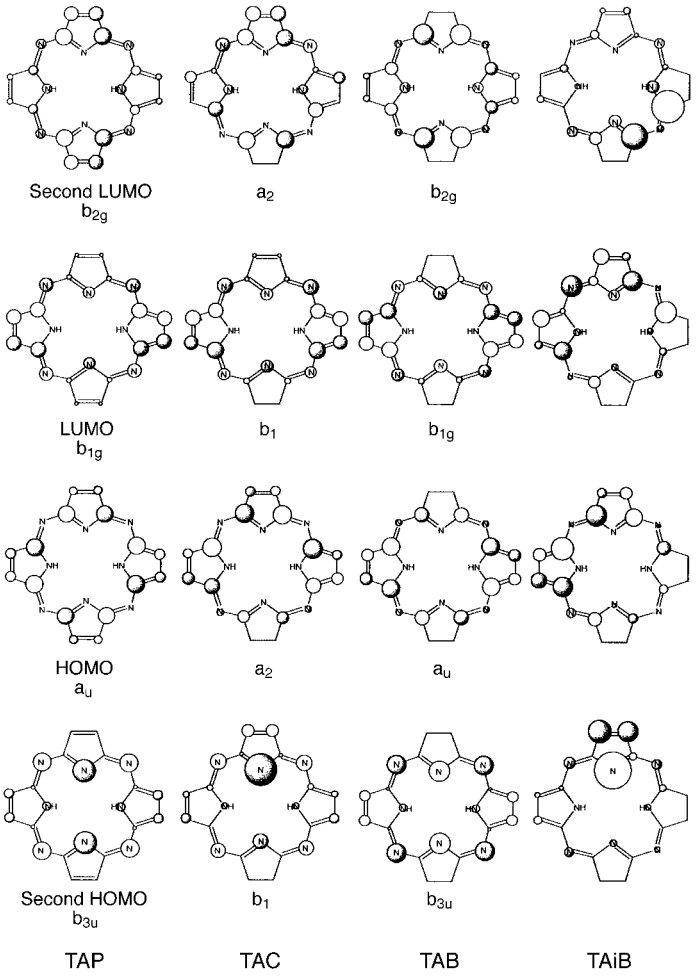

Figure 7. Four frontier orbitals of TAP, TAC, TAB, and TAiB. Only p_z orbitals are shown.

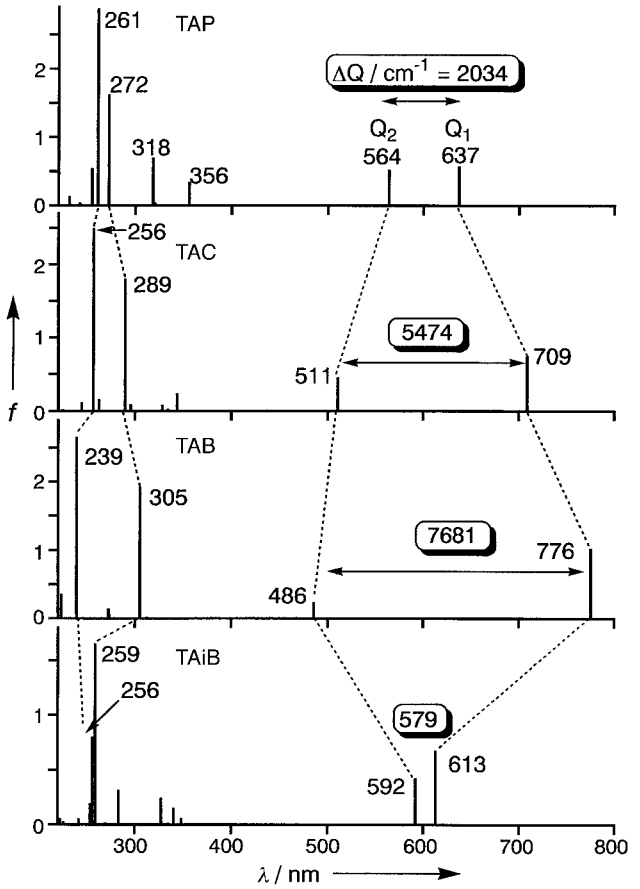

Figure 8. Absorption wavelengths and oscillator strengths obtained by CI calculations on TAP, TAC, TAB, and TAiB.

HOMO–LUMO transitions have nearly equal energy and intensity and are mixed by configurational interaction (CI) to produce the Q and Soret (B) bands.[31] The Q band is weaker than the Soret (B) band, since the Q band consists of the difference in transition dipole moments between the HOMO–LUMO and second HOMO–LUMO, while the Soret (B) band consists of the sum of these. In contrast, in TAP the second HOMO is strongly stabilized, so that the energy difference between the HOMO and second HOMO levels increases. Accordingly, CI is smaller, and the HOMO–LUMO transition mainly generates the Q band, while the second HOMO–LUMO transition constitutes the main part of the Soret band. With lowering of the molecular symmetry, the e_g LUMOs split into two nondegenerate orbitals, so that both the Q and Soret bands split into two bands. The shorter wavelength Q band component (Q2 band) and the longer wavelength component of the Soret (B) band approach each other and hence mix further by CI. Therefore, as in the case of porphyrins,[31] the intensity of the Q2 band becomes smaller than that of the Q1 band due to cancellation of the two components of the transition dipole moments.

The CI calculations help to interpret the absorption and MCD spectroscopic data more quantitatively (Figure 8 and Table 4), and the main results can be summarized as follows. 1) The Q bands of TAP, TAC, TAB, and TAiB are at 564 and 637 nm, 511, and 709 nm; 486 and 776 nm; and 592 and 613 nm, respectively. 2) The splitting of the Q band is 2034, 5474, 7681, and 579 cm^{-1}, respectively, in the above order. 3) The Q2 and Q1 transitions, with the exception of TAiB, are polarized in the *y* and *x* directions, respectively (the *x* axis is located along the N–H bonds). 4) The oscillator strengths of the Q2 and Q1 bands are 0.509 and 0.557; 0.445 and 0.735; 0.225 and 1.016; and 0.412 and 0.665, respectively, in the above order of compounds. These results are in good agreement with the trends observed experimentally.

The main electronic configurations of the Q1 bands of TAP, TAC, and TAB are the HOMO–LUMO and second HOMO–second LUMO configurations, whereby the ratios are 82 and 16% in TAP, 88 and 7% in TAC, and 90 and 8% in TAB, respectively, so that the purity of the HOMO–LUMO transition in the Q1 band increases with decreasing size of the π system. On the other hand, the Q2 bands consist mainly of the HOMO–second LUMO and second HOMO–LUMO electronic configurations, in which the ratios are 85 and 13% in TAP, 86 and 10% in TAC, and 80 and 20% in TAB, respectively. Accordingly, the electronic configurations of the Q2 bands mix more strongly than those of the Q1 bands with decreasing size of the π system. These calculated results are consistent with the qualitative interpretation obtained with the four-orbital models. In contrast, for TAiB, the contributions of the HOMO–LUMO and HOMO–second LUMO

Table 4. Calculated transition energies, oscillator strengths f, and configurations[a]

Energy [cm^{-1}]	λ [nm]	f	Polarization	Configurations[b]	
TAP					
15700	637	0.557	x	57–58 (81.8%)	56–59 (16.1%)
17730	564	0.509	y	57–59 (85.1%)	56–59 (16.1%)
28110	356	0.329	x	56–59 (45.5%)	54–58 (13.1%)
31400	318	0.680	y	56–58 (66.9%)	54–58 (23.4%)
36730	272	1.610	y	54–58 (64.8%) 56–58 (13.4%)	57–59 (6.3%)
38280	261	2.863	x	56–59 (32.8%) 57–58 (9.9%)	54–59 (50.4%)
TAC					
14100	709	0.735	x	58–59 (88.2%) 56–60 (2.5%)	57–60 (6.7%)
19580	511	0.445	y	58–60 (85.9%) 56–59 (3.4%)	57–59 (9.6%)
29080	344	0.224	y	57–59 (61.0%) 58–61 (14.0%)	58–60 (3.4%)
34560	289	1.788	y	57–59 (20.9%) 58–60 (9.4%)	56–59 (59.4%) 58–61 (4.4%)
38100	262	0.147	y	50–59 (85.3%)	53–60 (5.7%)
39010	256	2.480	x	56–60 (50.6%) 57–60 (19.6%)	58–59 (8.1%)
TAB					
12890	776	1.016	x	59–60 (89.8%)	58–61 (7.9%)
20570	486	0.225	y	59–61 (79.6%)	58–60 (19.5%)
32730	305	1.909	y	58–60 (77.7%)	59–61 (19.9%)
36670	273	0.127	x	59–64 (97.6%)	
41780	239	2.643	x	58–61 (77.0%) 59–68 (11.0%)	59–60 (7.6%)
TAiB					
16310	613	0.665		59–60 (69.7%)	59–61 (23.4%)
16890	592	0.412		59–60 (21.5%)	59–61 (73.3%)
29370	341	0.145		59–62 (68.7%)	58–60 (21.0%)
30580	327	0.233		59–63 (82.7%)	59–62 (4.4%)
35340	283	0.305		58–61 (75.1%)	58–60 (7.0%)
38620	259	1.644		57–60 (51.7%)	57–61 (22.7%)
39100	256	0.790		57–60 (27.7%)	57–61 (35.0%)

[a] Excited states with less than 4.85 eV and f greater than 0.12 are shown. [b] Orbital numbers 57, 58, 59, and 59 are HOMOs of TAP, TAC, TAB, and TAiB, respectively.

transitions are over 90% in the electronic configuration of both the Q1 and Q2 bands, while the contribution of the transition from the second HOMO is negligible (<2%). Hence, it is clear that the electronic structure of the Q state of TAiB is different from those of the other compounds.

The Soret band region is also reproduced correctly; estimated absorption wavelengths and oscillator strengths are included in Figure 8. The relatively sharp Soret band of TAP broadens on going to TAC, and in the case of TAB, the degree of splitting becomes sufficient to allow two clearly separated Soret bands to be seen (Figure 2). In contrast, the splitting of the Soret band of TAiB is so small that it appears as a single broad band (Figure 2). These trends are very similar to those found for the Q band, and indicate that the effect originates from the symmetry of the compounds. Two bands estimated at 356 and 318 nm for TAP correspond to transitions from low-lying orbitals to the LUMO and second LUMO. These are assigned to the shoulder at around 400 nm on the long-wavelength side of the main Soret band. Nakatsuji et al. assigned the main absorption peak at around 330 nm and the shoulder at around 400 nm as B_y (a transition polarized in the y direction) and B_x (a transition polarized in the x direction), respectively, without obtaining any experimental evidence.[53] However, taking into consideration our MCD results and CI calculations, it is clear that the 330 nm absorption band is composed of a superimposition of B_y and B_x transitions.

Excited triplet states: We now consider the unusual changes of the D value which accompanies the shrinkage of the π system. For the compounds in this study, there are no central metal atoms or substituents that cause spin-orbit coupling, so that the ZFS is due solely to magnetic dipole–dipole interactions. In general, the T1 states of Pcs and porphyrins without transition metals are π–π* in character, and are treated as a single configuration of the HOMO–LUMO transition. That is, the ZFS is interpreted through spin–spin interactions between the HOMO and LUMO electrons of the ligands. As described above, the HOMOs are significantly affected by hydrogenation of the pyrrole moiety, while the LUMOs are not. The contribution to the D value resulting from changes in the HOMO is considered as follows. Since there are almost no π electrons on the reduced pyrrole moiety, while the π electron density in the other regions of the HOMO simultaneously increases, the spin over the unreduced moiety of the HOMO interacts with the spin over the LUMO and thus increases the D value. On the other hand, the absence of interaction between the spin over the reduced pyrrole moiety of the HOMO and the spin over the LUMO leads to a decrease in D value. The experimental results show that the D decreases with increasing number of hydrogenated pyrrole rings, that is, the latter contribution to the D value is more important. The larger D value found experimentally for TAiB compared to TAP can be rationalized by considering that electrons of the HOMO and LUMO are localized over unreduced adjacent pyrrole rings.

To further quantify the above explanation, we have calculated the ZFS of T1 of these compounds under a half-point-charge approximation (Table 3).[54, 55] The D value decreases from 0.801 to 0.790 and to 0.647, while the E value increases from 0.152 to 0.188 and to 0.250, in the order of TAP, TAC, and TAB, respectively. The calculated D and E values (1.055 and 0.432, respectively) of TAiB are larger than those of the other compounds. Therefore, the calculated variation of D and E values is consistent with experiment and supports our argument. From the results, it is evident that the D value reflects the electron distribution in the T1 state.

0947-6539/02/0805-1088 $ 17.50+.50/0 *Chem. Eur. J.* **2002**, *8*, No. 5

Conclusion

Electronic absorption, MCD, fluorescence, and TRESR spectra, as well as cyclic voltammograms, of TAPs with hydrogenated pyrrole rings, namely, TAC, TAB, and TAiB, were recorded and compared with those of TAP. The splitting of the Q band increases, and the ratio of the shorter wavelength component Q2 to the longer wavelength component Q1 decreases, in the order TAP > TAC > TAB. For TAiB, a broad unsplit Q band appears near the center of the split Q band of TAP. In addition, comparison of the redox potentials indicates that, with the exception of TAiB, the LUMO level remains almost constant or is slightly stabilized, while the HOMO level becomes destabilized as the size of the π system decreases. Both the HOMO and the LUMO levels of TAiB are destabilized relative to those of TAP. The results were reproduced by MO calculations within the framework of the ZINDO/S Hamiltonian. A large splitting of the LUMO produces split Q bands in TAP, TAC, and TAB, while a small degree of splitting yields the unsplit broad Q band of TAiB (although this small splitting is experimentally detected by Faraday *B* term MCD). The fluorescence quantum yield of these compounds decreases remarkably with decreasing size of the π system. The experimentally obtained ZFS values are supported by calculations using the electronic distribution of the HOMO and LUMO under a half-point-charge approximation. In particular, the decrease in *D* value accompanying shrinkage of the π system has been reasonably explained as being caused by an interaction between the increased spin residing over the unreduced pyrrole moiety of the HOMO and the spin residing in the LUMO, although the *D* value generally increases in smaller π systems. Thus, we have succeeded in determining spectroscopic and electrochemical effects that accompany reduction and symmetry lowering of the π system of TAP.

Experimental Section

Chemicals: TAP was purchased from Aldrich Chemical Co. and purified by column chromatography on silica gel prior to use. The TAC and TAB used were those we reported previously.ö[13]

2,3:7,8-Bis[9,10-dihydro-2,6-di(*tert*-butyl)anthracene-9,10-diyl]tetraazaisobacteriochlorins (Ia, Ib): A mixture of tetraazaporphine[56] (60 mg, 0.19 mmol) and 2,6-di-*tert*-butylanthracene[57] (550 mg, 1.9 mmol) in *o*-dichlorobenzene (10 mL) was refluxed with stirring for 10 h. The reaction mixture was cooled to room temperature, filtered to remove excess 2,6-di-*tert*-butylanthracene, and the solvent was removed under reduced pressure. The residue was dissolved in a small amount of chloroform and purified by TLC on silica gel with chloroform/methanol (100/1) as eluent. The second and third violet fractions ($R_f = 0.71, 0.46$) were further purified individually by TLC on silica gel with chloroform as eluent for the second fraction and chloroform/ethyl acetate (10/1) for the third fraction, followed by precipitation from chloroform/methanol to give *trans*- and *cis*-TAiB. TAiB **Ia** (28 mg, 16.5 %): FAB MS: *m/z* (%): 895 (100) $[M+1]^+$, 604 (54) $[M - C_{22}H_{26}]^+$, 547 (22) $[M - C_{22}H_{26} - C_4H_9]^+$; elemental analysis (%) calcd for $C_{60}H_{62}N_8 \cdot H_2O$ (913.225): C 78.91, H 7.06, N 12.27; found: C 78.76, H 7.01, N 11.42; ^{1}H NMR (400 MHz, $CDCl_3$): $\delta = 0.60 - 0.64$ (d, 9H; *t*Bu), 0.74 – 0.77 (d, 9H; *t*Bu), 1.26 (s, 2H; NH), 1.36 – 1.40 (dd, 18H; *t*Bu), 4.19 – 4.45 (m, 4H; methine H), 5.03 – 5.29 (m, 4H; methine H), 5.53 – 5.65 (m, 2H; benzo H), 6.40 – 6.49 (m, 2H; benzo H), 6.68 – 6.79 (m, 2H; benzo H), 6.91 – 7.02 (m, 2H; benzo H), 7.27 – 7.31 (m, 2H; benzo H), 7.45 – 7.57 (m, 2H; benzo H), 7.61 – 7.65 (d, 2H; pyrrole H), 7.73 – 7.78 (m, 2H; pyrrole H). TAiB **Ib** (7 mg, 4.1 %): FAB MS: *m/z* (%): 895 (100) $[M+1]^+$, 604 (70) $[M - C_{22}H_{26}]^+$, 547 (44) $[M - C_{22}H_{26} - C_4H_9]^+$.

Measurements: Electronic absorption spectra were measured with a HITACHI U-3410 spectrophotometer. MCD spectra were recorded on a JASCO J-720 spectrodichrometer equipped with a JASCO electromagnet which produced magnetic fields of up to 1.09 T with parallel and antiparallel fields. Its magnitude is expressed in terms of molar ellipticity per tesla, $[\theta]_M/10^4\,\mathrm{deg\,mol^{-1}\,cm^{-3}\,cm^{-1}\,T^{-1}}$. Fluorescence spectra were recorded with a Hitachi F-4500 spectrofluorimeter. The absorbance at the excitation wavelength was less than 0.05. Fluorescence quantum yields Φ_f were determined by using metal-free tetraphenylporphyrine in benzene ($\Phi_f = 0.11$) as a standard,[58] by a comparative calibration method, using the same excitation wavelength and absorbance for the macrocycles and the calibrant, and the same emission energies. These spectroscopic measurements were made in chloroform.

Cyclic voltammetric measurements were performed with a Hokuto Denko HA-501 potentiostat/galvanostat connected to a Hokuto Denko HB-105 function generator. Differential pulse voltammetry experiments were performed with a Yanaco Model P-1100 electric analyzer. Conventional three-electrode cells were used, in which a glassy carbon electrode (area 0.07 cm^2) and a platinum wire were used as the working electrode and auxiliary electrode, respectively. The reference electrode was AgCl-coated Ag wire, corrected for junction potentials by internal reference to the ferrocenium/ferrocene (Fc^+/Fc) couple. In the solutions used, that is, in *o*-dichlorobenzene containing 0.1M tetrabutylammonium perchlorate (TBAP), the Fc^+/Fc couple was observed at approximately 0.52 ± 0.01 V versus AgCl/Ag. All of the electrochemical experiments were carried out under a dry nitrogen atmosphere.

TR-ESR measurements were carried out at 20 K on a Bruker ESP 300E spectrometer.[59] An Oxford ESR 900 cold gas flow system was used to control temperature. Samples were excited at 585 nm by a Lumonics HD 500 dye laser pumped with a Lumonics EX 500 excimer laser. The TR-ESR signals from the ESR unit were integrated by a LeCroy 9450A oscilloscope. For TR-ESR measurements, spectral-grade toluene was used as solvent, and samples were deaerated by the freeze – pump – thaw method.

For the structures used in the MO calculations, peripheral substituents were not taken into consideration. The π system of TAP was first optimized at the ZINDO/1 level of approximation.[50, 60] For TAC, TAB, and TAiB, it was assumed that they have almost the same structure as TAP, except for the hydrogenated pyrrole moieties. Therefore, only these moieties were optimized in the preoptimized TAP structure. The structures obtained in this way were then used to carry out CI calculations, performed within the framework of the ZINDO/S Hamiltonian.[50–52] The choice of configuration was based on energetic considerations, and all singly excited configurations up to 12 eV were included. For calculations of the ZFS parameters of T1 with a half-point-charge approximation,[54, 55] the LCAO coefficients of the HOMOs and LUMOs obtained in the MO calculations carried out within the framework of the PPP approximation[61–65] were used. In these calculations, structures were constructed by using the X-ray structural data of Pc [66–69] and by making the ring perfectly planar. Simulations of the T1 TRESR spectra were calculated by following a procedure already reported.[70]

Acknowledgements

This research was supported by a Grant-in-Aid for Scientific Research (B) No. 11440192 and the Scandinavia-Japan Sasakawa Foundation to N.K. E.L. and E.M. thank Moscow City Government and the Ministry of Science and Technology of Russia for financial support.

[1] *The Porphyrins* (Ed.: D. Dolphin), Academic Press, New York, **1978**.
[2] *The Porphyrin Handbook* (Eds.: K. M. Kadish, R. M. Smith, R. Guilard), Academic Press, New York, 2000.
[3] M. Gouterman, *J. Mol. Spectrosc.* **1961**, *6*, 138.
[4] *Phthalocyanine—Principles and Properties*, *Vols. I–IV* (Eds.: C. C. Leznoff, A. B. P. Lever), VCH, New York, **1989**, **1993**, **1993**, **1996**.
[5] *Phthalocyanines—Chemistry and Functions* (Eds.: H. Shirai, N. Kobayashi), IPC Publishers, Tokyo, **1997** (in Japanese).

[6] N. Kobayashi in *The Porphyrin Handbook*, *Vol. 2* (Eds.: K. M. Kadish, R. M. Smith, R. Guilard), Academic Press, New York, **2000**, Chap. 13, pp. 301 – 360.
[7] G. E. Ficken, R. P. Linstead, E. Stephen, M. Whalley, *J. Chem. Soc.* **1958**, 3879.
[8] N. S. Mani, L. S. Beall, A. J. P. White, D. J. Williams, A. G. M. Barrett, B. M. Hoffman, *J. Chem. Soc. Chem. Commun.* **1994**, 1943.
[9] A. G. Montalban, S. J. Lange, L. S. Beall, N. S. Mani, D. J. Williams, A. J. P. White, A. G. M. Barrett, B. M. Hoffman, *J. Org. Chem.* **1997**, *62*, 9284.
[10] A. G. Montalban, H. G. Meunier, R. B. Ostler, A. G. M. Barrett, B. M. Hoffman, G. Rumbles, *J. Phys. Chem. A* **1999**, *103*, 4352.
[11] H. Nie, C. L. Stern, A. G. M. Barrett, B. M. Hoffman, *Chem. Commun.* **1999**, 703.
[12] T. Hashimoto, Y. Choe, H. Nakano, K. Hirao, *J. Phys. Chem. A.* **1999**, *103*, 1894.
[13] E. A. Makarova, G. V. Korolyova, O. L. Tok, E. A. Luk'yanets, *J. Porphyrins Phthalocyanines* **2000**, *4*, 525.
[14] C. K. Chang, J. Fajer, *J. Am. Chem. Soc.* **1980**, *102*, 848.
[15] C. K. Chang, *Biochemisty* **1980**, *19*, 1971.
[16] A. M. Stolzenberg, T. Stershic, *Inorg. Chem.* **1987**, *26*, 1970.
[17] D. Chang, T. Malinski, A. Ulman, K. M. Kadish, *Inorg. Chem.* **1984**, *23*, 817.
[18] R. H. Felton in *The Porphyrins*, *Vol. V* (Ed.: D. Dolphin), Academic Press, New York, **1978**, Chap. 3, pp. 96 – 103.
[19] A. M. Stolzenberg, L. O. Spreer, R. H. Holm, *J. Am. Chem. Soc.* **1980**, *102*, 364.
[20] M. Gouterman in *The Porphyrins*, *Vol. 3* (Ed.: D. Dolphin), Academic Press, New York, **1978**, Chap. 1.
[21] J. D. Keegan, A. M. Stolzenberg, Y. Lu, R. E. Linder, G. Barth, A. Moscowitz, E. Bunnenberg, C. Djerassi, *J. Am. Chem. Soc.* **1982**, *104*, 4305.
[22] For porphyrins and TAPs with D_{4h} symmetry, the $\pi - \pi^*$ excited states (Q and B bands) are degenerate ($^1E_u = a_{1u} \times e_g = a_{2u} \times e_g$), and therefore the Q and B transitions give rise to dispersion-type Faraday *A* terms in the MCD spectra.
[23] If nonadjacent excited states apart from S_{1x} and S_{1y} (Q1 and Q2 transitions) are neglected, the Faraday *B* term for the first $S_{1x} - 0$ and the second $S_{1y} - 0$ transitions are given by Equation (1) where $\boldsymbol{m}$, $\boldsymbol{\mu}$, and ΔE represent off-diagonal matrix elements of magnetic and electric moment operators and energy gap between adjacent excited states, respectively.[24, 25] Therefore, the intensity of Faraday *B* terms is inversely related to the energy gap between the interacting transition states.

$$B_{0S1x} \sim Im(\boldsymbol{m}_{S1xS1y} \cdot \boldsymbol{\mu}_{0S1x}\boldsymbol{\mu}_{S1y0}/\Delta E_{S1xS1y}) = -B_{0S1y} \quad (1)$$

[24] P. J. Stephens, *Ann. Rev. Phys. Chem.* **1974**, *25*, 201.
[25] A. Tajiri, J. Winkler, *Z. Naturforsch. A* **1983**, *38*, 1263.
[26] M. J. Stillman, T. Nyokong in *The Phthalocyanines—Properties and Applications*, *Vol. 1* (Eds.: C. C. Leznoff, A. B. P. Lever), VCH, New York, **1989**, Chap. 3.
[27] N. Kobayashi, T. Ashida, K. Hiroya, T. Osa, *Chem. Lett.* **1992**, 1567
[28] N. Kobayashi, T. Ashida, T. Osa, *Chem. Lett.* **1992**, 2031.
[29] N. Kobayashi, T. Ashida, T. Osa, H. Konami, *Inorg. Chem.* **1994**, *33*, 1735.
[30] J. Mack, N. Kobayashi, C. C. Leznoff, M. J. Stillman, *Inorg. Chem.* **1997**, *36*, 5624.
[31] C. Weiss in *The Porphyrins*, *Vol. 3* (Ed.: D. Dolphin), Academic Press, New York, **1978**, Chap. 3.
[32] J. Michl, *J. Am. Chem. Soc.* **1978**, *100*, 6801.
[33] J. Michl, *J. Am. Chem. Soc.* **1978**, *100*, 6812.
[34] O. Gonen, H. Levanon, *J. Phys. Chem.* **1985**, *89*, 1637.
[35] O. Gonen, H. Levanon, *J. Chem. Phys.* **1986**, *84*, 4132.
[36] H. Levanon, A. Regev, T. Galili, M. Hugerat, C. K. Chang, J. Fajer, *J. Phys. Chem.* **1993**, *97*, 13198.
[37] A. Regev, T. Galili, C. J. Medforth, K. M. Smith, K. M. Barkigia, J. Fajer, H. Levanon, *J. Phys. Chem.* **1994**, *98*, 2520.
[38] K. Ishii, S. Yamauchi, Y. Ohba, M. Iwaizumi, I. Uchiyama, N. Hirota, K. Maruyama, A Osuka, *J. Phys. Chem.* **1994**, *98*, 9431.
[39] S. Yamauchi, Y. Matsukawa, Y. Ohba, M. Iwaizumi, *Inorg. Chem.* **1996**, *35*, 2910.
[40] K. Akiyama, S. Tero-Kubota, Y. Ikegami, *Chem. Phys. Lett.* **1991**, *185*, 65.
[41] R. Miyamoto, S. Yamauchi, N. Kobayashi, T. Osa, Y. Ohba, M. Iwaizumi, *Coord. Chem. Rev.* **1994**, *132*, 57.
[42] S. Yamauchi, H. Konami, K. Akiyama, M. Hatano, M. Iwaizumi, *Mol. Phys.* **1994**, *83*, 335.
[43] N. Kobayashi, M. Togashi, T. Osa, K. Ishii, S. Yamauchi, H. Hino, *J. Am. Chem. Soc.* **1996**, *118*, 1073.
[44] K. Ishii, Y. Hirose, N. Kobayashi, *J. Phys. Chem. A* **1999**, *103*, 1986.
[45] K. Ishii, N. Kobayashi, Y. Higashi, T. Osa, D. LeLievre, J. Simon, S. Yamauchi, *Chem. Commun.* **1999**, 969.
[46] K. Ishii, T. Ishizaki, N. Kobayashi, *J. Phys. Chem. A* **1999**, *103*, 6060.
[47] J. H. van der Waals, W. G. van Dorp, T. J. Schaafsma in *The Porphyrins*, *Vol. 4* (Ed.: D. Dolphin), Academic Press, New York, **1978**, Chap. 3.
[48] W. G. van Dorp, W. H. Schoemaker, M. Soma, J. H. van der Waals, *Mol. Phys.* **1975**, *30*, 1701.
[49] J. F. Kleibeuker, R. J. Platenkamp, T. J. Schaafsma, *Chem. Phys.* **1978**, *27*, 51.
[50] Hyper Chem. 5.1 Pro software package, Hypercube, Inc. Gainesville, FL, USA, **1997**.
[51] J. E. Ridley, M. C. Zerner, *Theor. Chim. Acta* **1976**, *42*, 223.
[52] A. D. Bacon, M. C. Zerner, *Theor. Chim. Acta* **1979**, *53*, 21.
[53] K. Toyota, J. Hasegawa, H. Nakatsuji, *Chem. Phys. Lett.* **1996**, *250*, 437.
[54] J. Higuchi, *J. Chem. Phys.* **1963**, *38*, 1237.
[55] S. Yamauchi, N. Hirota, J. Higuchi, *J. Phys. Chem.* **1988**, *92*, 2129.
[56] E. A. Makarova, G. V. Korolyova, E. A. Luk′yanets, *Zh. Obshch. Khim.* **1999**, *69*, 1356.
[57] T. A. Shatskaya, M. G. Galpern, V. R. Skvarchenko, E. A. Luk′yanets, *Zh. Obshch. Khim.* **1986**, *56*, 392.
[58] D. J. Quimby, F. Longo, *J. Am. Chem. Soc.* **1975**, *97*, 5111.
[59] K. Ishii, J. Fujisawa, A. Adachi, S. Yamauchi, N. Kobayashi, *J. Am. Chem. Soc.* **1998**, *120*, 3152.
[60] W. Anderson, W. D. Edwards, M. C. Zerner, *Inorg. Chem.* **1986**, *28*, 2728.
[61] R. Pariser, R. G. Parr, *J. Chem. Phys.* **1953**, *21*, 466, 767.
[62] J. A. Pople, *Trans. Faraday. Soc.* **1953**, *46*. 1375.
[63] S. Tokita, K. Matsuoka, Y. Kogo, K. Kihara, *Molecular Design of Functional Dyes: The PPP Method and Its Application*, Maruzen, Tokyo, **1990**.
[64] H. Hammond, *Theor. Chim. Acta* **1970**, *18*, 239.
[65] N. Mataga, K. Nishimoto, *Z. Phys. Chem. (Frankfurt am Main)* **1957**, *13*, 140.
[66] J. M. Robertson, I. Woodward, *J. Chem. Soc.* **1937**, 217.
[67] P. A. Barrett, C. E. Dent, R. P. Linstead, *J. Chem. Soc.* **1936**, 1719.
[68] C. J. Brown, *J. Chem. Soc. A* **1968**, 2488, 2494.
[69] J. E. Kirner, W. Dow, J. R. Scheidt, *Inorg. Chem.* **1976**, *15*, 1685.
[70] K. Tominaga, S. Yamauchi, N. Hirota, *J. Phys. Chem.* **1990**, *94*, 4425.

Received: May 25, 2001
Revised: October 22, 2001 [F3291]

  0947-6539/02/0805-1090 $ 17.50+.50/0